

Design and Testing of a Diamond-Shaped Four-Wheeled Gantry-like Sugarcane Cultivator

Qingting Liu¹ · Mojin Zhu¹ · Tao Wu¹ · Jiacheng Zhou¹ · Xiaoming Luo¹ · Tengfeng He¹ · Xiaoping Zou¹

Received: 10 December 2020 / Accepted: 26 February 2021 / Published online: 27 March 2021
© Society for Sugar Research & Promotion 2021

Abstract As there was a lack of high-ground-clearance sugarcane field management machinery, a diamond-shaped four-wheeled gantry-like cultivator was designed and developed. Both front and rear wheels of this machine were hydraulically driven and steered, with driven wheels on both sides. A gantry-like structure was used to connect the supports of the driven wheels and the main frame; the net passing height for the sugarcane underneath the gantry was 2400 mm. The wheel track could be adjusted from 2000 to 2800 mm to adapt to different row spacings. In this study, the designs of the key components, including the drive system, the driven wheels, the wheel track adjustment mechanism, the steering mechanism and the cultivator, were achieved. Simulation analysis on the stability of the cultivator was conducted by the kinetics software ADAMS. The results showed that the limit of the longitudinal slope angle and the cross slope angle of the proposed machine was 41.25° and 31.17°, respectively. In addition, the maximum driving speed of the vehicle, the minimum turning circle, the longitudinal slope angle, the cross slope angle and the maximum ridge height were determined experimentally on the open concrete floor. The results showed that the maximum driving speed of the vehicle was 13 km/h, its minimum turning circle was 7100 mm, the longitudinal slope angle and the cross slope angle was 8°, and the maximum height of the ridge was 160 mm.

Keyword Sugarcane · Rhomboid cultivator · Design · Simulation

Introduction

Sugarcane is a type of high-stalk base sugar crop. The mechanized cultivation uses a cultivator to carry out soil loosening, weeding, top dressing and trench ditch cultivation (Wang et al. 2013). The traditional manual cultivation method involves high labour intensity and high cost. Mechanized cultivation can increase production, reduce costs and lessen labour intensity (Liang 2003). To reduce planting costs, as well as increase and stabilize the income from planting, scholars have carried out research into the trial production of a sugarcane cultivator. The 3ZP-0.8 mini sugarcane cultivator that was developed by Guangxi Guigang Power Co., Ltd. utilizes a front and rear rotary tiller, is capable of reversible duplex operation, has low power consumption and is flexible; 3ZP-0.8 walks between two rows of sugarcane. However, when the row spacing of the sugarcane is ≥ 1.2 m, the use of the machine results in poor soil cultivation (Chen 2010). The 3ZSP-2 multifunctional sugarcane fertilizing and soil-cultivating machine was jointly developed by the Agricultural Machinery Research Institute at the China Academy of Tropical Agriculture and Guangxi Guigang Xijiang Machinery Co., Ltd. This machine is of good quality, but its equipment and the supporting tractors have only a relatively low ground clearance, thus making it unsuitable for the cultivation, fertilization and weeding operations of sugarcane in its middle growth period (Li et al. 2016). The four-wheeled diamond-shaped agricultural high ground clearance machine that was developed by Shandong Agricultural University uses a gantry structure that has

✉ Qingting Liu
qingting@scau.edu.cn

¹ South China Agricultural University, Wushan Road, Tianhe District, Guangzhou, Guangdong, China

high ground clearance; the university's researchers studied and designed its self-levelling system (Fan et al. 2016). Based on the patents that were filed, South China Agricultural University has developed two generations of diamond-shaped sugarcane cultivators and has also improved the design of its hydraulic walking system (Huang et al. 2017; Luo 2014). However, there have been only a few studies on the dynamic analysis of the chassis of a four-wheeled diamond-shaped gantry-like cultivator or the design of its key components. In this article, the requirements of sugarcane cultivation agronomy, the stability of the entire machine, the working environment and several other factors are comprehensively considered, and research into the design, performance analysis and experiments on a four-wheeled diamond-shaped sugarcane cultivator is presented.

Materials and Methods

Sugarcane Inter-tillage Cultivation Requirements

The agronomic requirement of sugarcane is “deep ploughing and shallow burying”; the depth of a planting ditch is 20–30 cm. After planting the cane seeds, the cane seeds are covered by a soil layer of 5–8 cm. The row spacing during sugarcane planting should meet the requirements of the sugarcane harvester's operation. A large harvester requires the planting row spacing to be ≥ 1.4 m, a medium-sized harvester requires the row spacing to be ≥ 1.2 m, and a small harvester requires the row spacing to be ≥ 1.0 m. When the cane seedlings grow 5 or 6 true leaves, combined with the first top dressing (tillering, adding fertilizer), inter-tillage weeding and small soil cultivation should be performed; this loosens the soil, improves soil aeration, removes weeds and creates good conditions for the sugarcane to grow. Sugarcane undergoes a jointing period. The average plant height of sugarcane plants can generally exceed 1.0 m, and the maximum width of the sugarcane ridges can reach 400 mm. Sugarcane needs the most nutrients when it grows large roots, large leaves and large stems. The amount of fertilizer absorbed accounts for more than 50% of the total amount of fertilizer absorbed, and the second top dressing should be carried out in a timely manner. Large-scale soil cultivation should be carried out to form turtle-shaped cane ridges with a height of 8–15 cm; this can help the machines cut into the soil during machine harvesting and can also prevent lodging at the later stages of growth. Sugarcane grows quickly during the jointing period; the existing cultivator that hangs behind the tractor often breaks the top of this faster growing sugarcane due to the insufficient ground clearance of the tractor. Therefore, the design of a high-ground-clearance cultivator is required

to be an effective measure in preventing the top of the sugarcane from being broken when cultivating the soil (Ou et al. 2018).

Based on the aforementioned inter-tillage agronomic requirements of sugarcane and in order to prevent the cultivator from damaging the sugarcane strain during its operation, the cultivator's wheel assembly that was designed has a maximum width of 600 mm, and the gantry has a height of at least 1.7 m. At the same time, the structure must be equipped with a corresponding adjustment mechanism so that it can adapt to a change in the line spacing of the sugarcane.

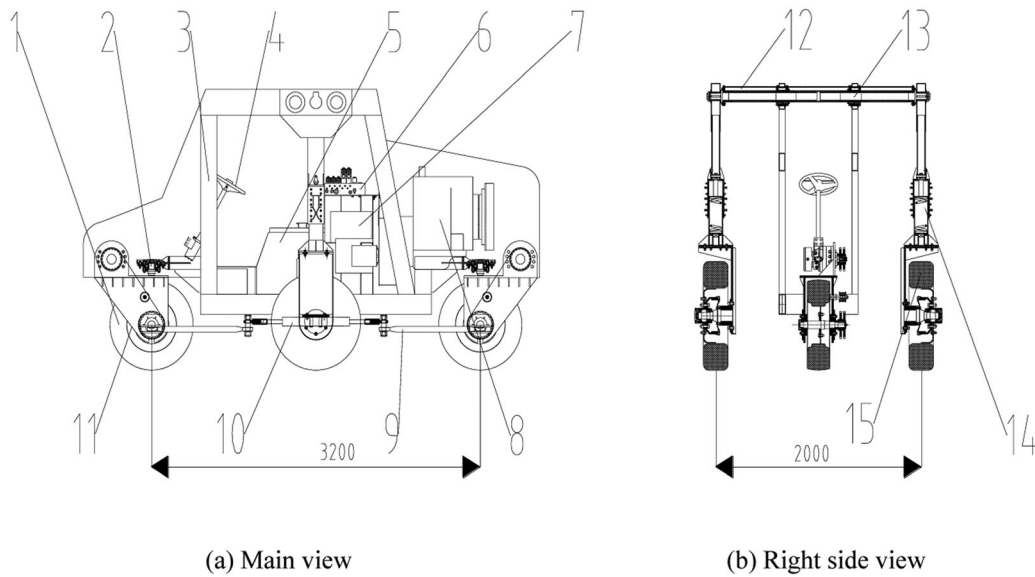
Design Requirements

The main areas where sugarcane cultivators work are hills and mountains; the road surface situation is complicated in these areas, and there are many sloping fields (Luo 2011). In addition, taking the agronomic requirements of sugarcane planting into consideration, a sugarcane cultivator requires strong supporting power, high ground clearance, good stability and somewhat flexible machinery to ensure that the machinery can meet the needs of sugarcane inter-tillage. The specific requirements of the cultivator are as follows:

1. Speed of 0–10 km/h;
2. Minimum turning circle ≤ 7500 mm;
3. Slope driving angle $\geq 8^\circ$;
4. Maximum ridge clearance height ≥ 150 mm;
5. Adjustable line spacing of 1.0 ~ 1.4 m;
6. Ability to clear sugarcane with a height of 1.5 m.

Structure of the Machine

The structural layout of the cultivator designed in the paper is shown in Fig. 1. The design refers to a patent for a “diamond-shaped four-wheel gantry-like high ground clearance cultivator”, patent No. CN 103650682 B. It is composed of an engine, a frame, a transfer case, a hydraulic motor, a chain, a hydraulic steering cylinder, a steering coupling lever, an arm, a telescopic cylinder for the arm, a spring shock absorber, the driven wheels, a hydraulic pump and other parts. The driven wheels are powered by hydraulic motors, and the front and rear wheels are used for steering. The rod steering system ensures that the front and rear wheels are turned synchronously and hydraulically. To achieve sufficient clearance height and be adaptable to a change in the sugarcane planting row spacing, a gantry-like structure was adopted (Qin et al. 2018). The hydraulic cylinder drive arm allows the driven wheels to extend outwards on both sides to adapt to different row spacings. The main structural parameters of the



1. Driven wheels, 2. Hydraulic motor, 3. Frame, 4. Steering wheel, 5. Hydraulic oil tank, 6. Hydraulic valves, 7. Fuel tank, 8. Engine, 9. Steering rod, 10. Steering cylinder, 11. Transmission chain, 12. Arm, 13. Telescopic cylinder, 14. Spring shock absorber, 15. Driven wheels,

Fig. 1 The structure of the cultivator

Table 1 The structural parameters of the cultivator

Parameters	Values
Dimensions (L × W × H), mm	4444 × 2410 × 2576
Structural quality, kg	4125
Wheel track, mm	2000–2800
Wheel base, mm	3200
Minimum ground clearance, mm	300
Gantry height, mm	2400

cultivator are listed in Table 1. Moreover, the cultivator has the capability to install the cultivator on the rear side of the supports for the driven wheels and the rear wheel base, as well as a spray and fertilizer application device on the front of the support to meet the needs of the cultivator.

1) Driven wheels, 2) hydraulic motor, 3) frame, 4) steering wheel, 5) hydraulic oil tank, 6) hydraulic valves, 7) fuel tank, 8) engine, 9) steering rod, 10) steering cylinder, 11) transmission chain, 12) arm, 13) telescopic cylinder, 14) spring shock absorber, 15) driven wheels,

Design of the System and its Key Components

Driving System

To improve the dynamic performance of the cultivator when it is driven in a field, the whole machine adopted a hydraulic drive for the front and rear wheels (Chen et al. 2016); this drive was coupled with chain transmission. The top speed on a flat road should reach 10 km/h, and the operating speed should reach 5 km/h. The slope it can be driven on was designed to be 8°, and the maximum uphill speed was set at 5 km/h.

The cultivator travels at a slow speed during operation; therefore, the effects of air resistance and acceleration resistance can be ignored, and the main forces acting on the cultivator include ramp resistance, tillage resistance and rolling resistance, as shown in Eqs. (1) ~ (2):

$$\sum F = F_f + F_i + F_R \tag{1}$$

$$\sum F = G\cos\alpha f + G\sin\alpha + F_R \tag{2}$$

The limit of ground adhesion is:

$$F_\phi = (F_{Z1} + F_{Z3})\phi \tag{3}$$

The range of the driving force of the cultivator is:

$$\sum F \leq F_t \leq F_\phi \quad (4)$$

where $\sum F$ (N) is the resistance acting on the whole machine; F_f (N) is the rolling resistance; F_i (N) is the slope resistance; F_R (N) is the tillage resistance, taken as 2 kN; G (N) is the force acting on the machine due to gravity; α ($^\circ$) is the ramp angle; F_ϕ (N) is the ground adhesion force; F_{Zi} (N) is the ground contact pressure of the i axle's wheel; f is the rolling resistance coefficient, which was taken as 0.16; ϕ is the ground adhesion coefficient, which was taken as 0.87; and F_{ti} (N) is the wheel driving force of the i axle.

A spring damper was installed above the driven wheels on both sides of the cultivator. The normal force of the driven wheels on both sides of the cultivator acting on the ground is equal to the sum of the spring force and the force due to gravity of the wheel assembly. The compression range of the designed spring was 63 mm; the spring force was calculated by multiplying the corresponding spring stiffness coefficient and adding the force due to gravity of the driven wheels. The sum of these two values resulted in the normal supporting force of the driven wheels. The mass of the entire machine was known, and the sum of the normal force received by the front and rear wheels was calculated to be 24255 N.

By substituting the relevant parameters into Eqs. (1), (2) and (3), the maximum resistance $\sum F$ acting on the whole machine was calculated as 14031 N, and the maximum adhesion force F_ϕ that the ground produces was 21101 N. Therefore, the driving force required for the wheels to produce was $14031 \text{ N} < F_t < 21101 \text{ N}$.

Hydraulic motor

Rotational speed of the hydraulic motor

The diameter of the driven wheels was 810 mm, and the speed range of the hydraulic motor could be determined according to the maximum and minimum driving speed of the whole machine. To meet the design speed requirements and take the low output speed of the hydraulic motor into consideration, a chain drive was used between the hydraulic motor and the driven wheels, and the initial chain transmission ratio $i = 1.2$. The speed range of the hydraulic motor can then be determined as follows:

$$\omega_m = \frac{v10^4}{\pi r} \quad (5)$$

where ω_m (r/min) is the rotational speed of the hydraulic motor, v (km/h) is the speed, and r (mm) is the radius of the driven wheels. By plugging the corresponding parameters into Eq. (5), it was found that the hydraulic motor's

minimum speed was 39.3 r/min, and its maximum speed was 78.6 r/min.

Torque of the hydraulic motor

The output torque of the hydraulic motor should be able to overcome the maximum resistance that occurs when the cultivator is operating. When driving up a 8° ramp, the resistance acting on the whole machine was 14031 N by Eq. (1–2).

The corresponding output torque of the motor can be calculated as follows:

$$T = \frac{F \cdot r}{ni\eta} \quad (6)$$

where F (N) is the driving force of the driven wheels; T (N·m) is the hydraulic motor's output torque; r (mm) is the radius of the driven wheels; n is the number of driven wheels; i is the transmission ratio of the drive chain; and η is the transmission efficiency of the hydraulic motor, which was taken to be 0.92.

It could then be calculated that the output torque of the hydraulic motor must be at least 2573 Nm.

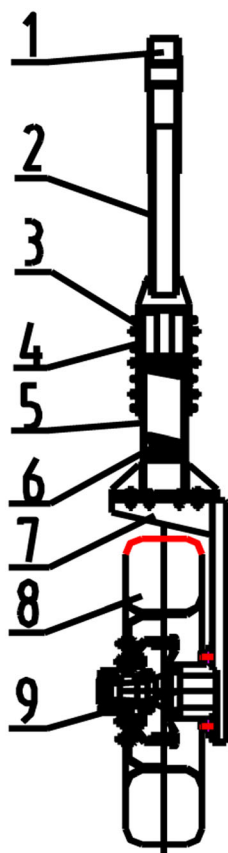
Driven Wheels' Mechanism

As shown in Fig. 2, the driven wheels on both sides of the cultivator adopted a candle suspension structure, and a spring damper was arranged in the middle of the component to ensure that the tires on both sides remained grounded at all times during operation. To reduce the wear of the spring damper from the longitudinal and lateral forces and to improve its stress condition, the spring damper was placed in a vertical channel composed of a wear plate and a sliding beam. An upper support beam was designed to be above the wear plate, which was connected to the table-shaped fixed plate. This fixed plate connected the arm and the driven wheels. The driven wheels' mounting plate was below the sliding beam, and the driven wheels were connected to the plate through the wheel's axle.

Wheelbase Adjustment Mechanism

As shown in Fig. 3, in order to adapt to a change in the spacing of sugarcane planting, the arm can adjust the distance between the driven wheels on both sides as well as the main frame through the use of the wheel track adjustment mechanism. The active component is the hydraulic cylinder inside the arm; this cylinder extends to drive the arm. The cylinders on both sides can be independently controlled. The external reinforced semicircular tube and the connecting tube bear the forces in all directions, while

Fig. 2 Structure of the driven wheels



links. The front and rear steering links were connected to the corresponding wheel steering shafts via the steering hinge seat. The angle between the axis of the hydraulic cylinder and the plane of longitudinal symmetry of the cultivator was 29°.

As shown in Fig. 4b, when the front and rear wheels are at their maximum steering angle, they produce a vertical line that is perpendicular to the wheels' plane through the front and rear wheel grounding centre points; the distance from the intersection of this vertical line and the axis of the middle driven wheels to the outer wheel's centre plane is the minimum steering radius (Zha et al. 2011; Huang et al. 2006). According to the geometric relationship, the turning circle *d* of the machine can be calculated as follows:

$$d = \frac{l}{\tan\delta} + B + B_t \tag{7}$$

where *l* (mm) is the wheelbase of the front and rear wheels, which was 3200 mm; δ (°) is the maximum steering angle of the wheels, which was set at 32°; *B_t* (mm) is the width of the middle tires, which was 220 mm; and *B* (mm) is the distance between the driven wheels, which was 2000 mm.

Substituting the relevant structural parameters into the above formula, the theoretical value of the turning circle of the whole machine could be obtained as 7341 mm.

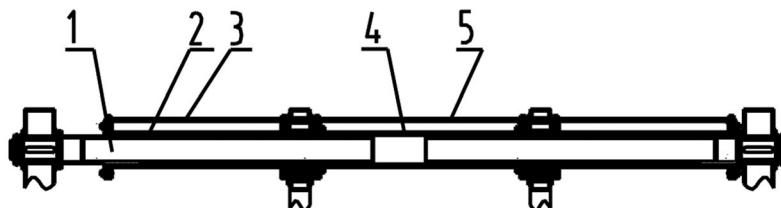
Operational Attachments

Agricultural tools can be attached to the cultivator, as shown in Fig. 5a, such as a harrow, a hydraulic cylinder, an active pull rod, a connecting rod and other components. There are three groups of corresponding suspension components for these attachments; these are installed on the mounting bases of the left, centre and right wheels. When the cultivator is not working in a field, the hydraulic cylinder can be used to lift the machine, and the rake group can be released during field work.

the hydraulic cylinder bears only the expansion and contraction lateral forces.

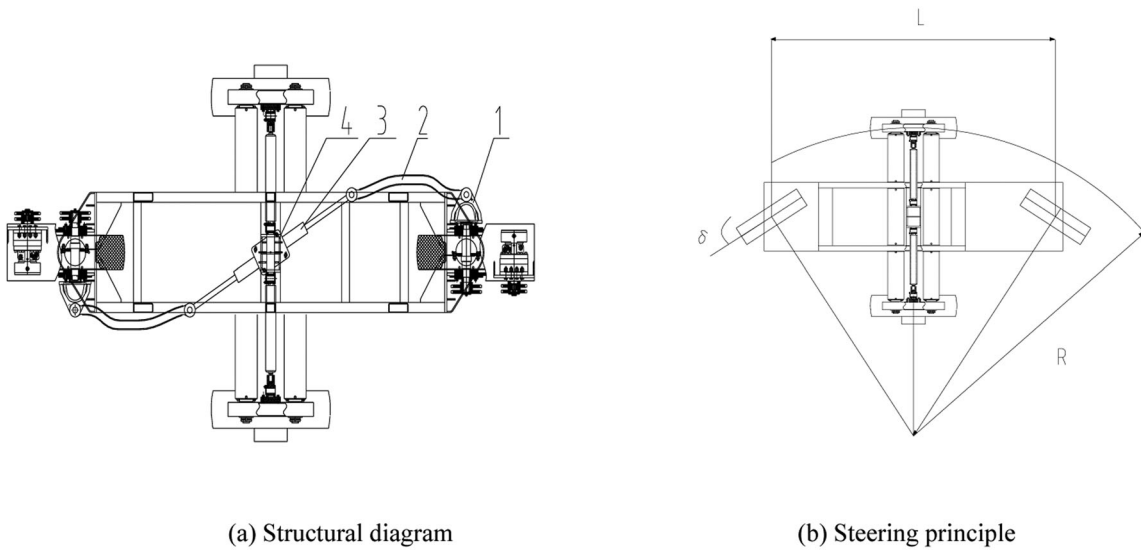
Steering Mechanism

The front and rear wheels of the diamond-shaped 4-wheel cultivator are steered; the front and rear wheels steer the cultivator using reverse deflection, and the steering centre is located on the extension of the axis of the two wheels. As shown in Fig. 4a, in order to achieve synchronous steering of the front and rear wheels, a double-acting hydraulic cylinder was used to connect the front and rear steering



1. Inner guide shaft, 2. Outer catheter, 3. Outer catheter reinforcing semi-circular tube, 4. Middle connecting tube, 5. Middle connecting tube reinforcing semicircular tube

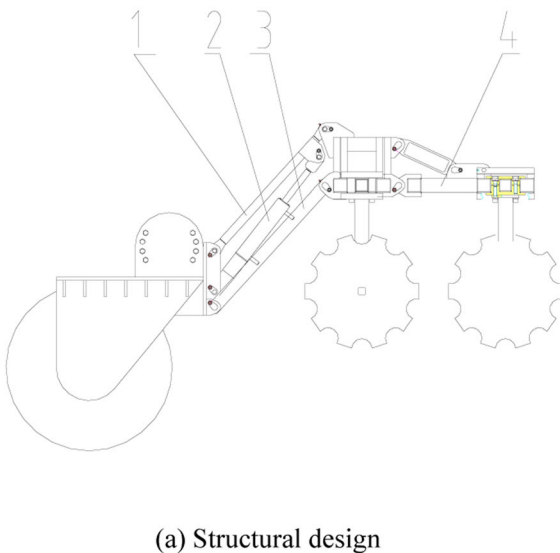
Fig. 3 Structural diagram of the wheelbase adjustment mechanism



1. Steering hinge seat 2. Steering connecting rod 3. Steering hydraulic cylinder 4. Hydraulic cylinder fixed seat

Note: L is the wheelbase of the front and rear wheels, mm; δ is the steering angle, °; R is the steering radius, mm.

Fig. 4 The steering mechanism. 1) Steering hinge seat, 2) steering connecting rod, 3) steering hydraulic cylinder, 4) hydraulic cylinder fixed seat. L is the wheelbase of the front and rear wheels, mm; δ is the steering angle, °; R is the steering radius, mm



1. Active pull rod 2. Suspension lifting hydraulic cylinder 3. Suspension connecting rod 4. Harrow group

Fig. 5 Structural diagram of the machine. 1) Active pull rod, 2) suspension lifting hydraulic cylinder, 3) suspension connecting rod, 4) harrow group

Chassis Performance Analysis

Ridge Crossing Performance

Many studies have been carried out on the performance of the traditional two-axle chassis design of agricultural machinery, mainly on the chassis’s steering performance, stability performance, etc. (Wang et al. 2017), but little research has been done on the ridge crossing performance of multi-axle agricultural vehicles. However, for the cultivator that was designed in this article, the first and third axle wheels were rigidly connected to the frame, and the second axle wheel was elastically connected to the frame. Due to the particular structure of the cultivator, a specific analysis was required.

The entire machine model was established using the three-dimensional CAD software CATIA, and the information about the centre of mass of the entire machine was measured in order to calculate the ridge crossing performance of the entire machine. The height of the centre of mass of the entire machine was measured in CATIA software, which was 1164 mm, and the centre of mass was located at the rear of the machine; its horizontal distance from the intermediate shaft was 182 mm.

When crossing a ridge, the speed of the cultivator is low; therefore, the problem can be simplified to a static problem. As shown in Fig. 6, the forces acting on the wheels when obstacles were encountered in the front, middle and rear wheels of the whole machine were analysed.

In Fig. 6, F_{Z1} (N) is the force normal to the road, acting on the front wheel as a result of the ridge; F_{Z2} (N) is the force normal to the road, acting on the centre wheel; F_{Z3} (N) is the force normal to the road, acting on the rear wheel; F_{t1} (N) is the force tangential to the road, acting on the front wheel; F_f (N) is the force tangential to the road, acting on the centre wheel; F_{t3} (N) is the force tangential to the road, acting on the rear wheel; G (N) is the force due to gravity acting on the vehicle; β ($^\circ$) is the inclination of the cab body; a ($^\circ$) is the angle between the wheel’s normal force and the road; ΔH (mm) is the height of the ridge; Δs (mm) is the distance from the centre of mass to the middle axis; and L (mm) is the wheelbase.

The deformation of the tires was ignored; then, the mechanical balance equations of the front, middle and rear wheels during the crossing of a ridge were established.

Front wheel ridge crossing model

$$\begin{cases} F_{Z1}\cos a = \phi F_{Z1}\sin a - fF_{Z2} + \phi F_{Z3} \\ F_{Z1}\sin a + \phi F_{Z1}\cos a + F_{Z2} + F_{Z3} = G \\ \phi F_{Z1} \frac{D}{2} + \left(\frac{l}{2} + \Delta s\right)G - fF_{Z2} \frac{D}{2} + \phi F_{Z3} \frac{D}{2} = F_{Z2} \frac{l}{2} + F_{Z3}l \end{cases} \tag{8}$$

Middle wheel ridge crossing model

$$\begin{cases} \phi F_{Z1} - fF_{Z2}\sin a + \phi F_{Z3} = F_{Z2}\cos a \\ F_{Z1} + F_{Z2}\sin a + F_{Z3} = G + fF_{Z2}\cos a \\ F_{Z1} \left(\frac{l}{2} \cos \beta - \frac{\Delta H}{2} \tan \beta\right) - fF_{Z2} \frac{D}{2} + Gl_2 \\ + \phi F_{Z1} \left(\frac{D}{2} - \Delta H\right) + \phi F_{Z3} \frac{D}{2} = F_{Z3}l_3 \\ l_2 = (H_g + \cot \beta \Delta s + \frac{\Delta H}{2 \cos \beta}) \sin \beta \\ l_3 = \left(\frac{l}{2} \cos \beta + \frac{\Delta H}{2} \tan \beta\right) \\ \sin \beta = \frac{\Delta H}{l} \end{cases} \tag{9}$$

Rear wheel ridge crossing model

$$\begin{cases} \phi F_{Z1} - fF_{Z2} + \phi F_{Z3}\sin a = F_{Z3}\cos a \\ F_{Z1} + F_{Z2} + F_{Z3}\sin a + \phi F_{Z3}\cos a = G \\ \phi F_{Z1} \left(\frac{D}{2} - \Delta H\right) + F_{Z1}l \cos \beta + \phi F_{Z3} \frac{D}{2} + F_{Z2} l_4 \\ - fF_{Z2} \left(\frac{D}{2} - \Delta H\right) = Gl_5 \\ l_4 = \frac{l}{2 \cos \beta} \sin 2\beta \\ l_5 = \left[\left(\frac{l}{2} - \Delta s\right) \cos \beta - \left(H_g - \frac{D}{2}\right) \sin \beta\right] \\ \sin \beta = \frac{\Delta H}{l} \end{cases} \tag{10}$$

$$\sin a = 1 - \frac{2\Delta H}{D} \tag{11}$$

where G (N) is the force due to gravity acting on the vehicle; β ($^\circ$) is the angle of the body of the vehicle; a ($^\circ$) is the angle between the wheel’s normal force and the ground; ΔH (mm) is the height of the ridge; Δs (mm) is the distance from the centre of mass of the vehicle to the middle axis; L (mm) is the wheelbase of the vehicle; D (mm) is the diameter of the wheels; L_2 (mm) is the horizontal distance between the centre of mass of the vehicle and the centre of the middle wheel when the middle wheel crosses the ridge; l_3 (mm) is the horizontal distance between the normal supporting force acting on the rear wheel and the centre of the middle wheel when the middle wheel crosses the ridge; l_4 (mm) is the horizontal distance between the normal force acting on the middle wheel and the centre of the rear wheel when the rear wheel crosses

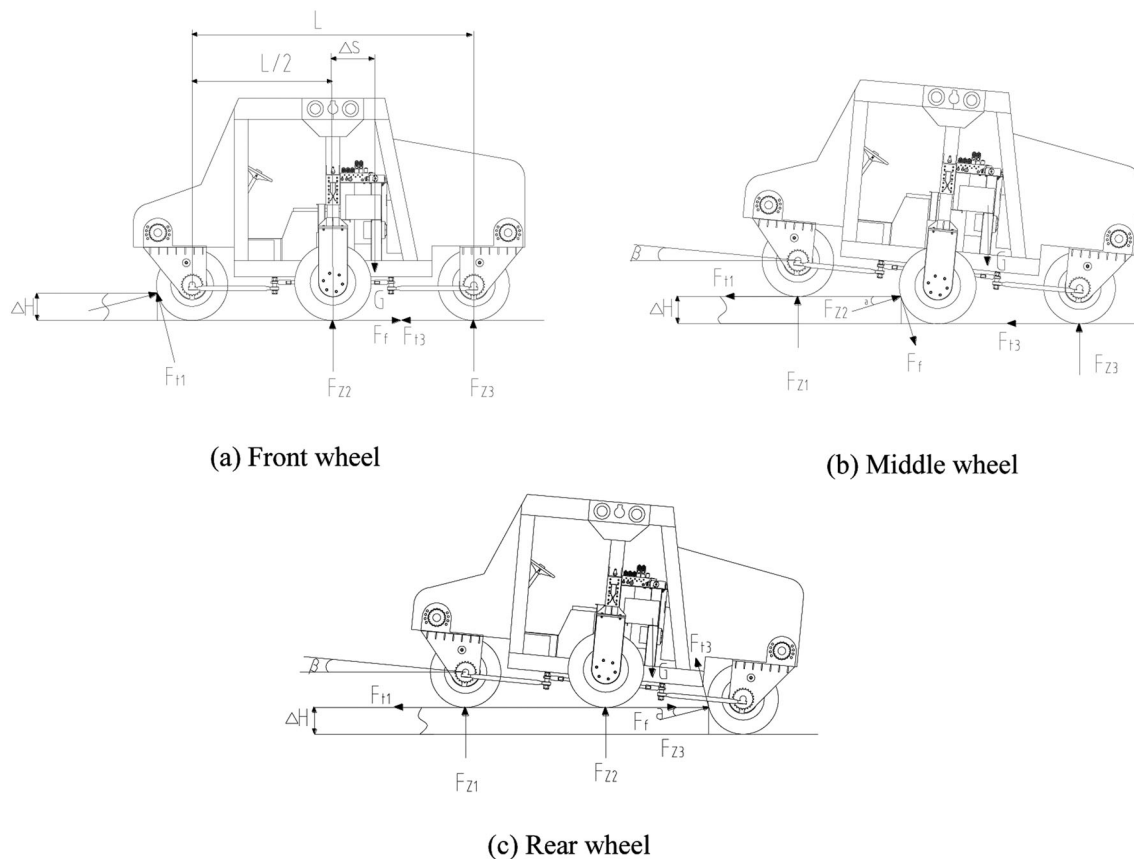


Fig. 6 Diagram of the cultivator crossing a ridge

over the ridge; l_5 (mm) is the horizontal distance between the centre of mass of the vehicle and the centre of the rear wheel when the rear wheel crosses the ridge; and H_g (mm) is the vertical height of the centre of mass of the vehicle.

Considering the influence of the expansion and contraction of the spring on the normal road force of the middle wheel during the process of crossing a ridge and assuming that the tire is in a pure rolling state when the machine is running at low speed, the change in the length of the spring can be calculated from the following equations:

$$\begin{cases} h = \frac{D}{2} [\sin(\omega t + a) - \sin a] \\ \sin\beta = \frac{h}{l} \\ \frac{h/2}{\cos\beta} = \Delta x \end{cases} \quad (12)$$

where h (mm) is the change in the height of the front wheel; ω ($^\circ/s$) is the angular velocity of the driven wheels; t (s) is time, s; and Δx (mm) is the spring deformation.

Correspondingly, the force acting on the middle wheel at different times when crossing a ridge can be written as:

$$F_{Z2} = m_i g + k(x \pm \Delta x) \cos\beta \quad (13)$$

where the sign of Δx (mm) is determined by either the extension or compression of the spring. F_{Z2} (N) is the force acting on the intermediate wheel; m_i (kg) is the mass of the wheel, which was 190 kg; $g = 9.8 \text{ m/s}^2$ is the acceleration due to gravity; and k (N/mm) is the stiffness of the spring damper.

The mechanical balance equations of the different axle shafts crossing the ridge and the deformation of the middle wheel springs were then combined to form a mathematical model of each axle shaft crossing a ridge. The problem of a traditional three-axle vehicle crossing a ridge is a statically indeterminate problem (Dang et al. 2014; Wei et al. 2011, 2019). However, during the cultivator’s progress, the normal force acting on the middle wheel changed with the expansion and contraction of the spring and the change in the body angle of the cultivator; this is a varying and quantifiable value. The calculated force values were put into the three-stage equation for the ridge crossing system. The simplified equation system has only three equations and three variables; therefore, the equation of the system can be solved. Due to the complexity of the calculation process, the SOLVE function in MATLAB was used to carry out the calculation, and the known structural

parameters were substituted to obtain the corresponding height of the ridge that was crossed.

The calculation results showed that the height of the ridge that could be crossed by the first axle was 426 mm, the height of the ridge that could be crossed by the second axle was 152 mm, and the height of the ridge that could be crossed by the third axle was 192 mm; therefore, the height of the ridge that was crossed for the entire machine was 152 mm, which meets the design requirements for the cultivator. It can be seen that, for the same adhesion coefficient, the height of the ridge that could be crossed, corresponding to the driven wheels, was lower. Although the current results meet the design requirements, when considering optimization of the whole machine, the whole machine could be designed as an all-wheel drive or the wheel radius could be enlarged in order to increase the height of the ridge that can be crossed.

Stability Performance of the Machine

The condition of the machine when working on the ramp is shown in Fig. 7. The rollover test is a relatively dangerous test for vehicles; at the critical overturning condition, it is easy for the whole machine to roll over and cause an accident. Using the kinematics software, the model of the whole machine was used for the rollover test simulation on both horizontal and vertical slopes, and the value corresponding to the working condition was obtained from the simulation; this value can be used to effectively evaluate the critical value of the cultivator and avoid the danger of rollover.

First of all, according to the characteristics of the designed model, the rollover model of the whole machine on both longitudinal and cross slopes was established. The impact of the suspension’s structure on the overturning performance must be considered (Mo 2009; Hao 2014; He 2004). The limit angle formula and the limit slip angle

formula of longitudinal and cross slope overturning were then established from the following equations:

$$\alpha_{limz} = \arctan(l/2 - \Delta s H_g) \tag{14}$$

$$\alpha_{limh} = \arctan(B/2 - H_g \sin\theta H_g \cos\theta) \tag{15}$$

$$\alpha \leq \arctan(\varphi) \tag{16}$$

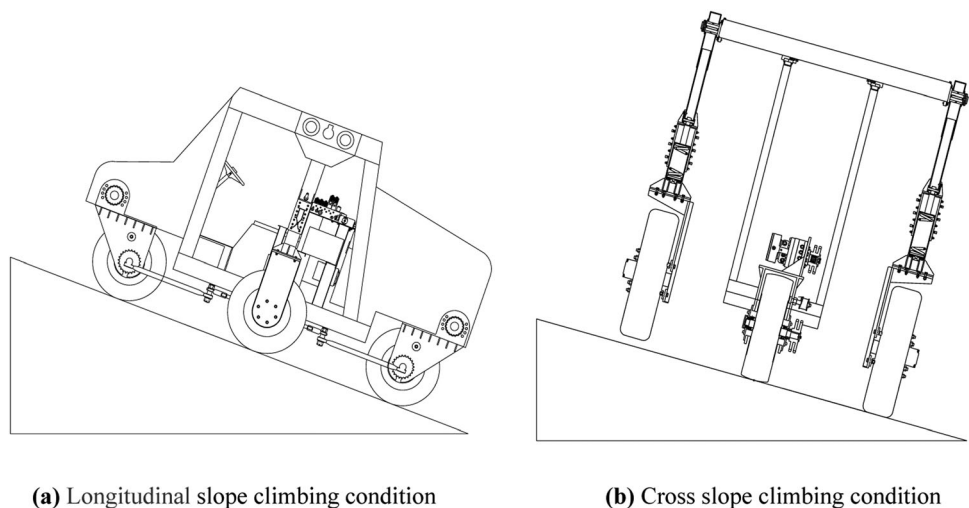
where $\alpha_{limz}(\circ)$ is the overturning limit angle for a longitudinal slope; α_{limh} is the overturning limit angle for a cross slope; $H_g(\text{mm})$ is the vertical height of the centre of mass of the vehicle; and $\theta(\circ)$ is the body roll angle, taken to be $14^\circ/g$.

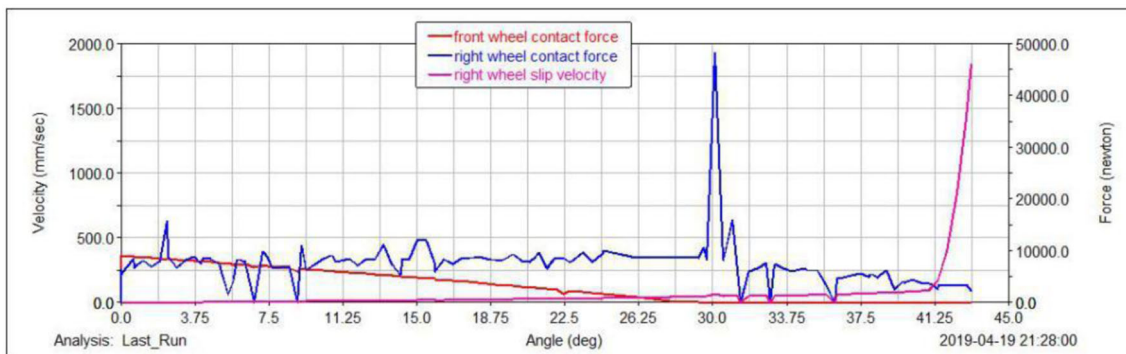
The relevant parameters were then substituted into the above formulas to obtain the following values: $\alpha_{limz} = 50.7^\circ$, $\alpha_{limh} = 30.7^\circ$, and $\alpha \leq 41^\circ$. Therefore, from the theoretical calculations, it was found that the longitudinal slope overturning angle was 41° , and the cross slope overturning angle was 30.7° .

After the mathematical model had been established, the kinematics software ADAMS was used for the analysis (Li 2014; He et al., 2018). The 3D model of the whole assembly created in CATIA was converted into the STP format and imported into ADAMS software. The materials were added to the corresponding parts, and motion pairs were added to constrain the corresponding parts. The friction coefficient between the tire and the ground was set to 0.16, and the adhesion coefficient was set to 0.87.

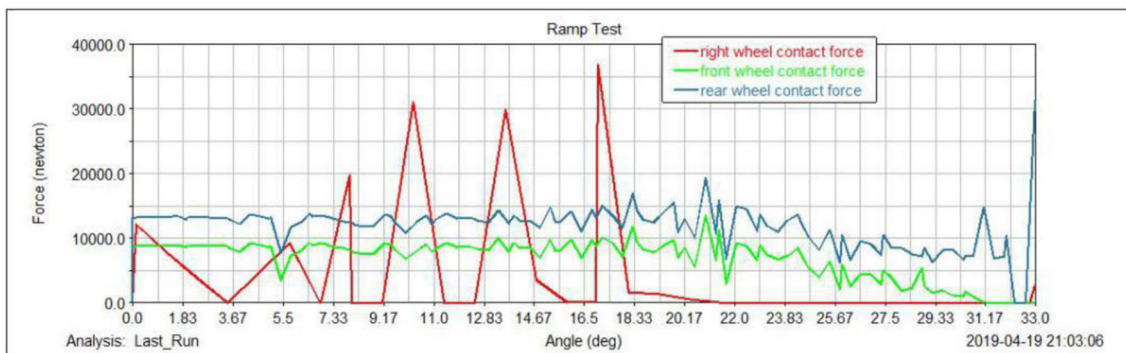
To simulate the slope stability of the whole machine, the machine was placed on a horizontal platform, the horizontal platform was rotated at $0.3^\circ/\text{s}$ around one axis, and the simulation was stopped when the cultivator overturned. The ramp limit angle of the cultivator was based on the angle when the contact force between the tire and the horizontal platform was 0 and when the relative slip speed was significant.

Fig. 7 Schematic diagram of the cultivator driving on a ramp





(a) Longitudinal slope climbing conditions



(b) Cross slope climbing conditions

Fig. 8 Simulation diagram of the slope climbing conditions**Fig. 9** Experimental test diagram

As shown in Fig. 8. The results of the simulation have shown that for longitudinal slopes, the ground pressure of the front wheels was 0 at an angle of 27° , and the whole machine significantly slipped at an angle of 41.25° . Although there was still ground pressure on the middle driven wheel at this point, it could no longer keep the machine stable. For cross slopes, the contact pressure of the right wheel was 0 at a slope angle of 22° , and the contact pressure of the front wheel was 0 at an angle of 31.17° . Therefore, the longitudinal slope limit angle of the machine was 41.25° , and the cross slope limit angle was 31.17° .

Comparing the simulation results with the theoretical calculation values, it can be seen that the theoretical calculation values were close to the simulation results; therefore, this can be used as a reference for the design process.

Results and Discussion

As shown in Fig. 9. To make an objective evaluation of the whole machine and assess its performance, on April 16, 2019, a test was conducted in the open space of the Hanniu

Table 2 Experimental test results

Parameters	Test results	Technical requirements
Driving speed, km/h	0–13	0–10
Minimum turning circle, mm	7.1	≤ 7.5
Longitudinal slope climbing angle, °	8	≥ 8
Cross slope climbing angle, °	8	≥ 8
Maximum ridge crossing height, mm	160	≥ 150
Wheel track adjustment range, mm	2000 ~ 2800	$\geq 2000 \sim 2600$

Agricultural Machinery Co., Ltd. in Conghua District, Guangzhou City, Guangdong Province.

The following instruments were used in the test: (1) electronic stopwatch (accuracy 0.01 s); (2) tape measure (0–5 m, accuracy 1 mm); and (3) inclinometer (accuracy 0.1°).

Experimental Method

The performance of the various components of the machine was tested separately. When testing the driving speed, a test distance of 20 m was measured, and a starting buffer area of 10 m and a braking buffer area of 20 m were cleared. The machine accelerated into the test area at full speed. The mechanical tire marker started timing when the machine entered the test area and stopped when the marker reached the 20 m line, and the time was recorded. The test was performed six times, the speeds were calculated separately, and then, the average value was taken.

When testing the minimum turning circle, the machine moved at low speed, and the steering wheel was turned as far as it could go. The tester moved with the machine at the position of the outer tire and sprayed lime powder along the trajectory of the tire until the lime powder formed a closed circle, and then, the diameter of the circle was measured.

When testing the cross-ridge height, a block of a certain height was placed in the path of the machine to form an obstacle. To prevent the block from moving, the block was fixed to the ground. The machine was driven towards the obstacle, and it was deemed to have passed the obstacle when all four wheels were past the obstacle.

When testing the machine on a slope, a slope was chosen that met the test criteria, and the machine was considered to have passed if it could drive up the slope.

Test Results and Analysis

Test results are shown in Table 2. The test results showed that the operating speed and the minimum turning circle of the machine met the design requirements, and they were close to the theoretical calculation and the results from the simulation. The tests were constrained by the local environment, as the maximum slope of a ramp that could be found at the test site was 8°; therefore, this could not be used for the test of the limit angle. Nevertheless, the driving test on the existing slope met the design requirements. The difference between the height of the ridge and the theoretical value during the ridge test was small; thus, the rationality of the theoretical analysis was confirmed.

Discussion

According to the test results shown in Table 2, the performance of the cultivator in the field could be expected to be as follows:

The suitable range of the row space of the sugarcane for the cultivator was from 1000 to 1400 mm due to its wheel track adjustment range of 2000–2800 mm, as shown in Table 2.

The longitudinal slope and cross slope of a sugarcane field should both be less than 8° for the cultivator, according to the test results shown in Table 2.

The cultivator could pass a height of 160 mm, according to its maximum ridge crossing height shown in Table 2.

The ground speed of the cultivator when cultivating a sugarcane field should be tested further using field tests.

Conclusions

A diamond layout four-wheeled gantry-like sugarcane cultivator was developed in this paper.

Through the use of the dynamic software ADAMS, the simulation results showed that the cultivator's maximum climbing angle and lateral slope limit angle were 41.25° and 31.17°, respectively. On the cement concrete road of the factory, the experimental test results showed that the cultivator's speed, minimum turning circle, slope climbing limit angle, cross slope limit angle, maximum ridge crossing height and the adjustment range of the wheel track were 0–13 km/h, 7100 mm, 8°, 8°, 160 mm, and from 2000 to 2800 mm, respectively. These results have shown that the cultivator was able to meet the performance design requirements.

Acknowledgements This research was supported by Science and Technology Program of Guangzhou (201807010084), National Key

R&D Program of China (2016YFD0701202; 2018YFD0701105), Guangdong Provincial Team of Technical System Innovation for Sugarcane Sisal Industry (2019KJ104-11) and Sugar Industry Technical System Post Project of China (CARS-170402).

Declarations

Conflict of interest Authors declare that there is no conflict of interest and the work described has not been published before.

References

- Chen, X. 2010. Research and development of jiuling 3ZP_0.8 sugarcane cultivator. *Guangxi Agricultural Mechanization* 2010 (4): 28–30.
- Chen, S., D. Yuefeng, B. Xie, Z. Song, E. Mao, and Y. Chen. 2016. Design and performance analysis of drive system for high clearance self-propelled corn detasseling machine. *Transactions of the Chinese Society of Agricultural Engineering* 32 (22): 10–17.
- Dang, X.Z., L.H. Zhang, J.T. Yue, and X.C. Qu. 2014. The obstacle-jump problem of multi-axle vehicles. *Automotive Engineering* 36 (01): 119–124.
- Fan, G.Q., X.H. Zhang, J.X. Wang, H.M. Feng, Q.L. Yang, and F.T. Sun. 2016. Design and experiment of four-wheeled diamond-shaped agricultural high-gap work machine. *Transactions of the Chinese Society for Agricultural Machinery* 47 (02): 84–89.
- Hao, J.X. 2014. Analysis of suspension roll center and its application in chassis adjustment. *Journal of University of Shanghai for Science and Technology* 36 (05): 507–510.
- He, Y.J. 2004. *Design of independent suspension drive axle with single longitudinal arm transverse torsion bar*. Changsha: Hunan University.
- He, P., W.X. Ma, E.P. Zhao, X.Q. Lu, and X. Feng. 2018. Design and physical model test of the body leveling system of wheeled tractors in hilly mountains. *Transactions of the Chinese Society of Agricultural Engineering* 34 (14): 36–44.
- Huang, Z., and Z.H. Zhong. 2006. Analysis of steering performance of diamond new concept car. *Journal of Hunan University (Natural Sciences)* 2006 (06): 46–50.
- Huang, M., D.K. Zheng, D.T. Yang, and Q.T. Liu. 2017. Study on synchrony of rhomboid self-propelled chassis of sugarcane cultivator based on AMESim. *Journal of Agricultural Mechanization Research* 39 (06): 7–12.
- Li, Z.G. 2014. *Adams introduction and examples 2nd edition*. Beijing: National Defense Industry Press.
- Li, M., T. Zhang, X.H. Dong, C. Wang, Z.J. Niu, C. Ge, and L.J. Wei. 2016. Parameter optimization of 3ZSP-2 sugar cane intertillage fertilizer feeder scraper type fertilizer discharging device. *Transactions of the Chinese Society of Agricultural Engineering* 32 (23): 36–42.
- Liang, Z.X. 2003. Discussion on the development of sugarcane production mechanization. *Chinese Agricultural Mechanization* 2003 (02): 14–18.
- Luo, X.W. 2011. Reflections on the development of agricultural mechanization in hilly areas. *Popularization of Agricultural Machinery Science and Technology* 2011 (02): 17–20.
- Luo, X.M. 2014. *Design of chassis for rhomboid four-wheel gantry frame high ground clearance cultivator*. Guangzhou: South China Agricultural University.
- Mo, X.H. 2009. *Analysis and optimization of the manipulation dynamics of diamond-like vehicles*. Changsha: Hunan University.
- Ou, Y.G., and Q.T. Liu. 2018. *Study on sugarcane production mechanization*. Zhenjiang: Jiangsu University Press.
- Qin, W.H., H.M. Zhang, D.F. Zhong, Y.W. Zhao, and J.M. Ma. 2018. Development status of agricultural overhead work vehicle technology. *Agricultural Engineering* 8 (07): 5–11.
- Wang, J.L., X.J. Wang, S.L. Cao, and M. Wang. 2013. Research status and development trend of tillage fertilization machinery technology. *Anhui Agricultural Science* 41 (04): 1814–1816.
- Wang, J.W., H. Tang, H.G. Shen, H.C. Bai, and M.J. Na. 2017. Design and experiment of multi-functional power chassis for high-altitude waist-type paddy field. *Transactions of the Chinese Society of Agricultural Engineering* 33 (16): 32–40.
- Wei, D.G., Y.G. Ou, D.T. Yang, and Q.T. Liu. 2011. Dynamic distribution of axle load in multi-bridge driven vehicles over obstacles. *Transactions of the Chinese Society for Agricultural Machinery* 42 (02): 39–42.
- Wei, D.G., J.W. Song, W.M. Ju, P.B. Wu, G. Ju, X.F. Gao, and X.H. Chen. 2019. Study on the obstacle performance of heavy goods vehicles considering tire elasticity. *Automotive Engineering* 41 (01): 75–79.
- Zha, Y.F., Z.H. Zhong, and X.L. Yan. 2011. Analysis of steering performance of diamond-like vehicles based on flexible dynamics. *China Mechanical Engineering* 22 (02): 247–251.

Publisher's Note Springer Nature remains neutral with regard to jurisdictional claims in published maps and institutional affiliations.